

From Microscopic to Macroscopic Traffic Models

Dirk Helbing^{1,2}

¹ II. Institute of Theoretical Physics, University of Stuttgart, Pfaffenwaldring 57/III, 70550 Stuttgart, Germany

² Department of Fluid Mechanics and Heat Transfer, Tel Aviv University, Tel Aviv, 69978, Israel

Abstract. The paper presents a systematic derivation of macroscopic equations for freeway traffic flow from an Enskog-like kinetic approach. The resulting fluid-dynamic traffic equations for the spatial density, average velocity, and velocity variance of vehicles are compared to equations, which can be obtained from a microscopic force model of individual vehicle motion. Simulation results of the models are confronted with empirical traffic data.

1 Introduction

During the last five years, modelling and simulating traffic dynamics has found a large and rapidly growing interest in physics. This is due to

1. similarities of traffic dynamics with flows of gases, fluids, and granular media,
2. instability phenomena and critical behavior of traffic (cf. Fig. 1),
3. interesting applications of cellular automata and molecular dynamics simulation methods,
4. the need of efficient traffic optimization methods in order to keep or increase the level of mobility.

Usually, one distinguishes three levels of modelling: The microscopic level of description delineates the dynamics of the single driver-vehicle units [1], [2], [3], [4], [5]. This allows to consider different vehicle characteristics and driving styles, so that many of these models aim at a high-fidelity description of traffic flow, e.g. [3], [5]. They are mostly used for detail studies (e.g. of on-ramp traffic, bottlenecks, effects of traffic optimization measures), but they consume an enormous amount of CPU time due to the large number of variables involved. An alternative approach are cellular automata, which allow to simulate a minimal model of traffic dynamics faster than real-time [6], [7], [8], [9].

Computational efficiency can also be reached by macroscopic traffic models, but at a higher degree of accuracy [10], [11], [12], [13], [5]. Macroscopic traffic models consist of equations for a few aggregate quantities like the spatial density ρ , the average velocity V , and (in some cases) additional velocity moments. These equations are similar to fluid-dynamic equations, but some fundamental differences with respect to the dynamics of ordinary fluids have recently been recognized [5], [13]. For congested conditions, their detailed form is not at all

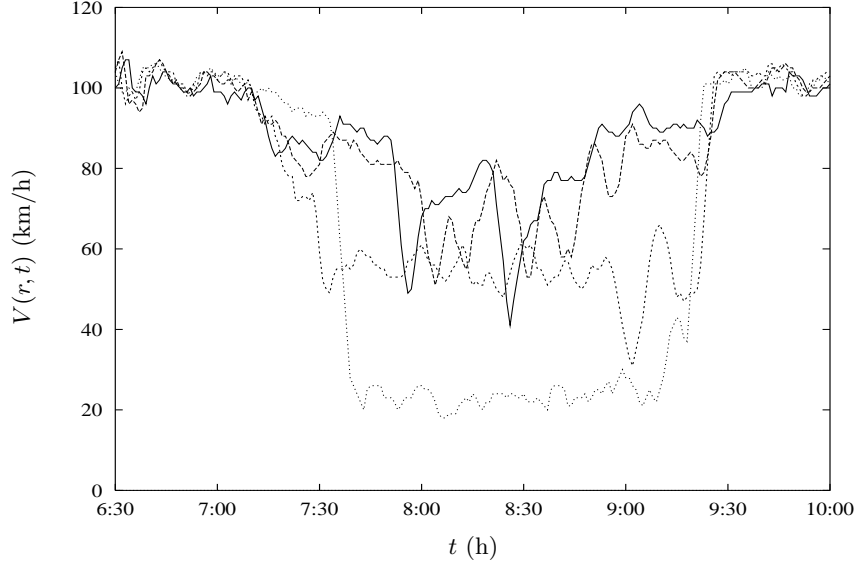


Fig. 1. Temporal evolution of the average velocity $V(r, t)$ at subsequent cross-sections of the Dutch highway A9 from Haarlem to Amsterdam at October 14, 1994 (five minute averages of single vehicle data) [14], [5]. The prescribed speed limit is 120 km/h. We observe a breakdown of velocity during the rush hours between 7:30 am and 9:30 am due to the overloading of the highway at $r = r_0 := 41.8$ km (\cdots). At the subsequent cross-sections the traffic situation recovers ($- -$: $r = r_0 + 1$ km; $-$: $r = r_0 + 2.2$ km; $—$: $r = r_0 + 4.2$ km). Nevertheless, the amplitudes of the small velocity fluctuations at r_0 become larger and larger, leading to so-called stop-and-go waves.

obvious. Therefore, it has been suggested to derive the macroscopic traffic equations from a kinetic, i.e. mesoscopic level of description, which delineates the spatio-temporal evolution of the velocity distribution [5], [13], [15], [16], [17], [18].

2 Enskog-like Kinetic Traffic Model

In the following, we define the coarse-grained phase-space density $\tilde{\rho}(r, v, t)$ of vehicles per lane with velocity v at place r and time t by

$$\tilde{\rho}(r, v, t) := \frac{1}{(2\Delta r)(2\Delta v)} \sum_{\alpha} \int_{r-\Delta r}^{r+\Delta r} dr' \int_{v-\Delta v}^{v+\Delta v} dv' \delta(r' - r_{\alpha}(t)) \delta(v' - v_{\alpha}(t)). \quad (1)$$

$r_{\alpha}(t)$ is the location and $v_{\alpha}(t)$ the velocity of vehicle α at time t . We do not distinguish different lanes, here, although this is possible [5], [19]. Instead, we treat the overall cross section of an n -lane freeway in an effective way [5], [20].

Let us assume an acceleration equation of the form

$$\frac{dv_\alpha}{dt} = f_0(v_\alpha) + \sum_{\beta(\neq\alpha)} f_{\alpha\beta}(r_\alpha, v_\alpha, r_\beta, v_\beta) + \xi_\alpha(t), \quad (2)$$

where the function

$$f_0(v_\alpha) := \frac{V_0 - v_\alpha(t)}{\tau} \quad (3)$$

describes an adaptation of the actual velocity $v_\alpha(t)$ to the desired velocity V_0 within a (possibly density-dependent) relaxation time τ . The second term in (2) delineates the effect of interactions with vehicles β , and $\xi_\alpha(t)$ reflects velocity fluctuations due to imperfect driving. We will assume $\langle \xi_\alpha(t) \xi_\beta(t') \rangle = 2D \delta_{\alpha\beta} \delta(t-t')$, where the diffusion function D is density- and velocity-dependent [5], [13], [26]. For reasons of simplicity, the desired velocity V_0 and the relaxation time τ were taken identical for all vehicles, but it is also possible to generalize this model [16], [17], [18].

From (1) and (2), the following dynamical equation for the phase-space density can be derived:

$$\frac{\partial \tilde{\rho}}{\partial t} + \frac{\partial(\tilde{\rho}v)}{\partial r} + \frac{\partial}{\partial v} [\tilde{\rho} f_0(v)] = \left(\frac{\partial \tilde{\rho}}{\partial t} \right)_{\text{fl}} + \left(\frac{\partial \tilde{\rho}}{\partial t} \right)_{\text{int}}. \quad (4)$$

The fluctuation term gives a contribution

$$\left(\frac{\partial \tilde{\rho}}{\partial t} \right)_{\text{fl}} = \frac{\partial^2(\tilde{\rho}D)}{\partial v^2}. \quad (5)$$

In addition, we have used the abbreviation

$$\left(\frac{\partial \tilde{\rho}}{\partial t} \right)_{\text{int}} := -\frac{\partial}{\partial v} (\tilde{\rho} f_{\text{int}}) \quad (6)$$

with the average interaction force

$$f_{\text{int}}(r, v, t) := \frac{1}{4\tilde{\rho} \Delta r \Delta v} \sum_{\alpha \neq \beta} \int_{r-\Delta r}^{r+\Delta r} dr' \int_{v-\Delta v}^{v+\Delta v} dv' f_{\alpha\beta} \delta(r' - r_\alpha(t)) \delta(v' - v_\alpha(t)). \quad (7)$$

The interaction term (6) reflects deceleration processes. In analogy to the Enskog theory of dense gases [21] and granular media [22], [23], [24], but with an interaction law typical for vehicles [5], [13], it is approximated by

$$\left(\frac{\partial \tilde{\rho}}{\partial t} \right)_{\text{int}} = (1-p) \chi(r+l, t) \mathcal{B}(v) \quad (8)$$

with the Boltzmann-like interaction function

$$\begin{aligned} \mathcal{B}(v) = & \int_{w>v} dw (w - v) \tilde{\rho}(r, w, t) \tilde{\rho}(r + s, v, t) \\ & - \int_{v>w} dw (v - w) \tilde{\rho}(r, v, t) \tilde{\rho}(r + s, w, t). \end{aligned} \quad (9)$$

According to this, the phase-space density $\tilde{\rho}(r, v, t)$ increases due to deceleration of vehicles with velocities $w > v$, which cannot overtake vehicles with velocity v . The density-dependent probability of immediate overtaking is represented by p . A decrease of the phase-space density $\tilde{\rho}(r, v, t)$ is caused by interactions of vehicles with velocity v with slower vehicles driving with velocities $w < v$. The corresponding interaction rates are proportional to the relative velocity $|v - w|$ and to the phase space densities of both interacting vehicles. By $s(V) = l_0 + l(V)$ (\approx vehicle length + safe distance) it is taken into account that the distance of interacting vehicles is given by their velocity-dependent space requirements. These cause an increase of the interaction rate, which is described by the pair correlation function $\chi(r) = [1 - \rho(r, t)s]^{-1}$ at the 'interaction point' $r + l$. A more detailed discussion of the above kinetic traffic model is presented elsewhere [5], [13].

Now, we will focus on the the macroscopic equations for the spatial density

$$\rho(r, t) = \int dv \tilde{\rho}(r, v, t), \quad (10)$$

the average velocity

$$V(r, t) = \int dv v \frac{\tilde{\rho}(r, v, t)}{\rho(r, t)}, \quad (11)$$

and the velocity variance

$$\theta(r, t) = \int dv [v - V(r, t)]^2 \frac{\tilde{\rho}(r, v, t)}{\rho(r, t)}. \quad (12)$$

These are obtained by multiplying the kinetic equation with v^k and integrating with respect to v . In order to obtain a closed system of equations, we assume that the velocity distribution $P(v; r, t)$ has a Gaussian form, i.e.

$$P(v; r, t) := \frac{\tilde{\rho}(r, v, t)}{\rho(r, t)} = \frac{e^{-[v - V(r, t)]^2 / [2\theta(r, t)]}}{\sqrt{2\pi\theta(r, t)}}. \quad (13)$$

According to empirical data, this approximation is well justified (cf. Figs. 2 and 3).

After some straightforward calculations, the following equations are obtained:

$$\frac{\partial \rho}{\partial t} + \frac{\partial(\rho V)}{\partial r} = 0, \quad (14)$$

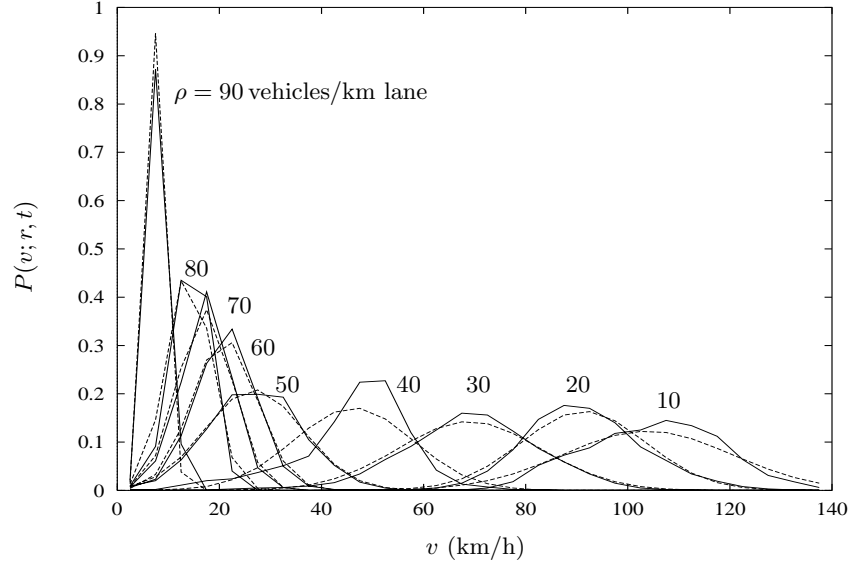


Fig. 2. Comparison of empirical velocity distributions at different densities (—) with frequency polygons of grouped Gaussian velocity distributions with the same mean value and variance (---) [25]. A significant deviation of the empirical relations from the respective discrete Gaussian approximations is only found at a density of $\rho = 40$ vehicles/km lane, where the temporal averaging period of $T = 2$ min may have been too long due to rapid stop-and-go waves.

$$\frac{\partial(\rho V)}{\partial t} + \frac{\partial}{\partial r}[\rho(V^2 + \theta)] = \frac{\rho}{\tau}(V_0 - V) + (1 - p)\chi(r + l, t) \int dv v \mathcal{B}(v), \quad (15)$$

$$\begin{aligned} \frac{\partial}{\partial t}[\rho(V^2 + \theta)] + \frac{\partial}{\partial r}[\rho(V^3 + 3V\theta)] &= \frac{2\rho}{\tau}(V_0 V + \tau D - V^2 - \theta) \\ &+ (1 - p)\chi(r + l, t) \int dv v^2 \mathcal{B}(v). \end{aligned} \quad (16)$$

Equations (14) to (16) are similar to the Euler equations of ordinary fluids. In particular, the density equation (14) agrees with the continuity equation, reflecting that the number of vehicles is conserved (on a circular road). However, equations (15) and (16) contain some additional terms compared to the hydrodynamic equations for momentum density and energy density, which are essential for the instability of traffic flow. The respective first terms on the right-hand sides of (15) and (16) originate from the acceleration towards the desired velocity V_0 and from velocity fluctuations. The respective last terms reflect interaction (deceleration) effects. In contrast to ordinary fluids, they do not vanish, since vehicular interactions do not conserve momentum and energy.

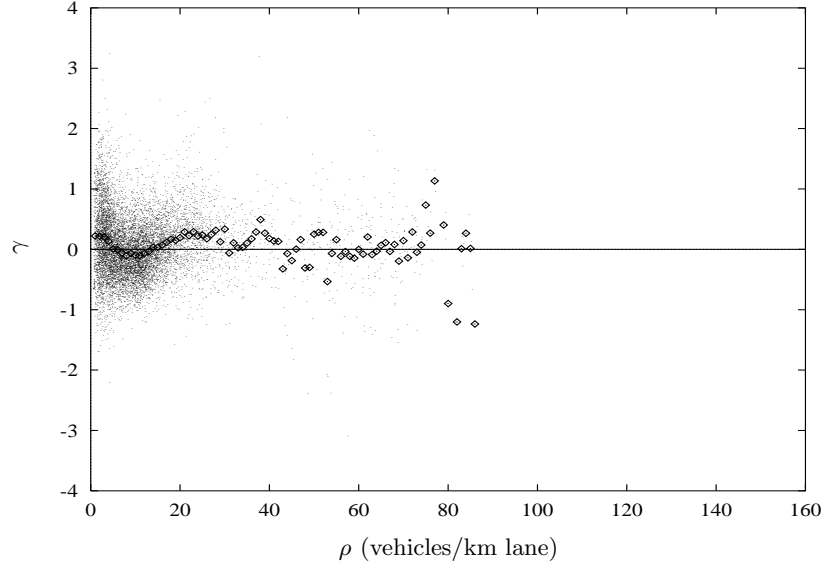


Fig. 3. Density-dependence of the skewness γ of the velocity distribution (\cdot : 1-minute data; \diamond : respective mean values) [25]. The large variation of the 1-minute data at low densities is due to the small number of vehicles which pass a cross section during the time interval $T = 1$ min, whereas the large variation of their mean values at high densities comes from the few 1-minute data, over which could be averaged. The 1-minute data of the skewness scatter around the zero line (—) and mostly lie between -1 and 1 , so that it is negligible most of the time.

To obtain the explicit form of the interaction terms, one has to carry out a number of lengthy calculations. Using the abbreviations

$$\rho_+(r, t) := \rho(r + s, t), \quad V_+(r, t) := V(r + s, t), \quad \theta_+(r, t) := \theta(r + s, t), \quad (17)$$

and introducing the Gaussian error function

$$\Phi(x) = \int_{-\infty}^x dy \frac{e^{-y^2/2}}{\sqrt{2\pi}}, \quad (18)$$

one finally finds

$$\begin{aligned} \int dv v \mathcal{B}(v) = -\rho \rho_+ \left\{ \left[(\theta + \theta_+) + (V - V_+)^2 \right] \Phi \left(\frac{V - V_+}{\sqrt{\theta + \theta_+}} \right) \right. \\ \left. + (V - V_+)(\theta + \theta_+) \frac{e^{-(V - V_+)^2/[2(\theta + \theta_+)]}}{\sqrt{2\pi(\theta + \theta_+)}} \right\} \end{aligned} \quad (19)$$

and

$$\begin{aligned} \int dv v^2 \mathcal{B}(v) = & -2\rho\rho_+(\theta - \theta_+) \left[(\theta + \theta_+) \frac{e^{-(V-V_+)^2/[2(\theta+\theta_+)]}}{\sqrt{2\pi(\theta + \theta_+)}} \right. \\ & \left. + (V - V_+) \Phi\left(\frac{V - V_+}{\sqrt{\theta + \theta_+}}\right) \right] + (V + V_+) \int dv v \mathcal{B}(v). \end{aligned} \quad (20)$$

The macroscopic traffic equations (14) to (16) were written as equations for fluxes with sink/source terms (the terms on the right-hand side). The flux representation is very advantageous, since many numerical integration algorithms have been developed for this type of partial differential equations. However, due to (19) and (20), the flux representation is non-local. This is caused by the finite space requirements of cars, i.e. a driver reacts to another car already at a certain distance. As a consequence, the non-local interaction terms imply viscosity effects, among other things. To see this, we expand them up to second order. Neglecting products of spatial derivatives, we get the continuity equation

$$\frac{\partial \rho}{\partial t} + V \frac{\partial \rho}{\partial r} = -\rho \frac{\partial V}{\partial r}, \quad (21)$$

the velocity equation

$$\begin{aligned} \frac{\partial V}{\partial t} + V \frac{\partial V}{\partial r} = & a_1 \frac{\partial \rho}{\partial r} + a_2 \frac{\partial V}{\partial r} + a_3 \frac{\partial \theta}{\partial r} \\ & + b_1 \frac{\partial^2 \rho}{\partial r^2} + b_2 \frac{\partial^2 V}{\partial r^2} + b_3 \frac{\partial^2 \theta}{\partial r^2} + \frac{V_e - V}{\tau}, \end{aligned} \quad (22)$$

and the variance equation

$$\begin{aligned} \frac{\partial \theta}{\partial t} + V \frac{\partial \theta}{\partial r} = & c_1 \frac{\partial \rho}{\partial r} + c_2 \frac{\partial V}{\partial r} + c_3 \frac{\partial \theta}{\partial r} \\ & + d_1 \frac{\partial^2 \rho}{\partial r^2} + d_2 \frac{\partial^2 V}{\partial r^2} + d_3 \frac{\partial^2 \theta}{\partial r^2} + \frac{2(\theta_e - \theta)}{\tau} \end{aligned} \quad (23)$$

(which corresponds to the equation of heat conduction in ordinary fluids). Here, we have used the abbreviations

$$\begin{aligned} a_1 = & -\left[\frac{1}{\rho} + (1-p)\chi s(1 + \rho\chi l)\right]\theta, & a_2 = & (1-p)\chi\rho\left(2s\sqrt{\frac{\theta}{\pi}} - \rho\theta\chi\frac{l^2}{V}\right), \\ a_3 = & -\left[1 + (1-p)\rho\chi\frac{s}{2}\right], & b_1 = & -(1-p)\chi s\left(\frac{s}{2} + \rho\chi\frac{l^2}{2}\right)\theta, \\ b_2 = & (1-p)\chi\rho\left(s^2\sqrt{\frac{\theta}{\pi}} - \rho\theta\chi\frac{l^3}{2V}\right), & b_3 = & -(1-p)\chi\rho\frac{s^2}{4}, \\ c_2 = & -[2 + (1-p)\chi\rho s]\theta, & c_3 = & 2(1-p)\chi\rho s\sqrt{\frac{\theta}{\pi}}, \\ d_2 = & -(1-p)\chi\rho s^2\frac{\theta}{2}, & d_3 = & (1-p)\chi\rho s^2\sqrt{\frac{\theta}{\pi}}, \end{aligned} \quad (24)$$

and

$$V_e = V_0 - \tau(1-p)\rho\chi\theta, \quad \theta_e = \tau D. \quad (25)$$

Note that $c_1 = 0$ and $d_1 = 0$, which is a consequence of the assumed interaction law of vehicles. It is one of the advantages of a kinetic derivation of macroscopic traffic equations, that the above functions can be analytically calculated. For example, we have obtained an expression for the equilibrium velocity V_e . According to (25), it is given by the desired velocity V_0 , diminished by a term due to decelerating interactions. The latter is proportional to the vehicle density and to the velocity variance, which is very plausible. The function $\partial\mathcal{P}/\partial\rho := -\rho a_1$ can be interpreted as the partial derivative of the “traffic pressure” \mathcal{P} with respect to density. The quantity $\eta := \rho b_2$ has the meaning of a viscosity, which smoothes out sudden spatial changes of the velocity profile $V(r, t)$. Both quantities are non-negative and diverge at maximum density $\rho_{\max} := 1/l_0$, as it should be for reasons of consistency [5], [13]. Previous macroscopic traffic models did not describe these important facts correctly, since they have neglected the terms in (24) which explicitly contain l or s . Therefore, they are not valid for high vehicle densities, i.e. for congested conditions. Finally, note that it is possible to calculate Navier-Stokes corrections of the coefficients a_i , b_i , c_i , and d_i [26].

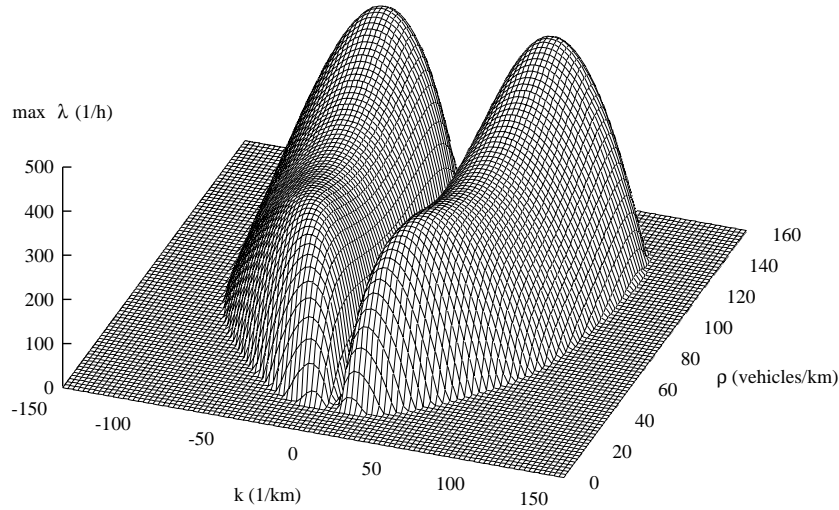


Fig. 4. Instability diagram for the Euler-like macroscopic traffic equations, including the dynamic variance equation [26].

According to our approximations, equations (21) to (23) are valid for small gradients of ρ , V , and θ . Therefore, they allow to investigate the evolution of small disturbances of the (stationary and spatially homogeneous) equilibrium solution. Figure 4 depicts the result of a linear instability analysis, showing that traffic flow is only stable at small and extreme densities as well as large wave numbers $|k|$ (i.e. small wave lengths $\ell = 2\pi/|k|$). This is in agreement with empirical findings.

The instability diagram is obtained by

1. assuming a small periodic perturbation $\delta g(r, t) = g_0 \exp[ikr + (\lambda + i\omega)t]$ of the macroscopic traffic quantities $g \in \{\rho, V, \theta\}$ relative to the stationary and spatially homogeneous equilibrium solution $g_e(\rho)$ (g_0 being the amplitude, k the wave number, λ the growth rate, and ω the frequency of the perturbation),
2. inserting $g(r, t) = g_e + \delta g(r, t)$ into the macroscopic traffic equations,
3. neglecting quadratic terms in the small perturbations $\delta g(r, t) \ll g_e$,
4. determining the three complex eigenvalues $\tilde{\lambda} = \lambda + i\omega$ of the linearized equations in dependence of ρ and k .

An explicit example for this procedure is discussed in [5], [13]. Equilibrium traffic flow is unstable if at least one of the growth rates is positive, i.e. $\max \lambda > 0$. Therefore, the instability diagram shows $\max \lambda(k, \rho)$ if this is greater than zero, otherwise 0. Figure 5 depicts a simulation result which demonstrates emerging stop-and-go traffic.

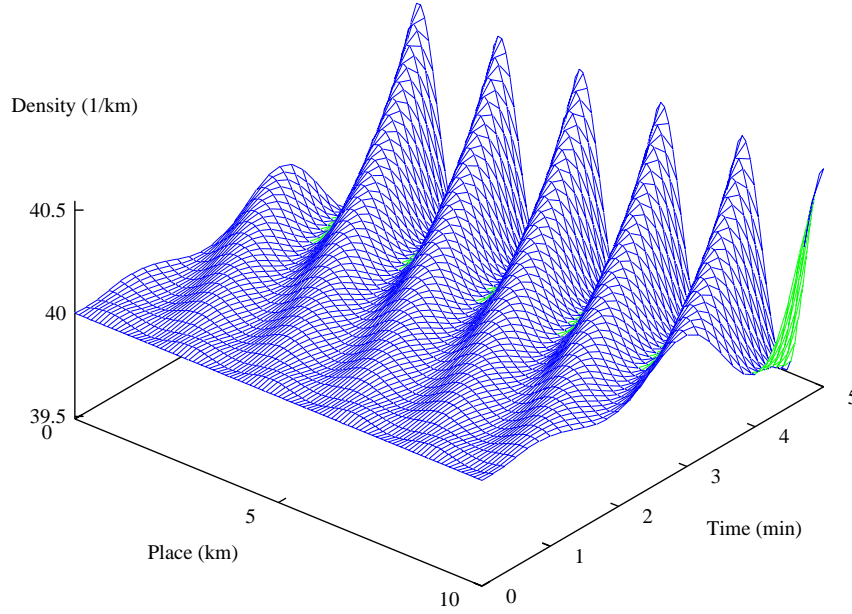


Fig. 5. Above a certain density, traffic flow is unstable. This gives rise to the development of stop-and-go waves. In the represented simulation, we applied periodic boundary conditions (which corresponds to a circular road).

2.1 Non-linear Phenomena

As a consequence of the inherent non-linearity of the macroscopic traffic equations, they display the self-organization of a number of collective patterns of mo-

tion. This includes the formation of density clusters (‘traffic jams’), anti-clusters, dipole layers, cascades of density clusters (‘stop-and-go traffic’), and merging of density clusters. Moreover, one finds subcritical instabilities and non-linear wave selection phenomena [11], [12].

3 An Alternative Approach

The Boltzmann-like formula (9) for vehicle interactions implicitly assumes, that deceleration maneuvers happen instantaneously. This approximation is only valid, if the average duration of deceleration maneuvers is considerably smaller than the time scale of the macroscopic traffic dynamics. However, one can also derive fluid-dynamic traffic equations without this assumption. We will illustrate this for a one-lane microscopic traffic model without possibilities of overtaking.

3.1 A Concrete Microscopic Model

Let us start with the *social force model* of vehicle dynamics, given by $dr_\alpha/dt = v_\alpha(t)$ and

$$\frac{dv_\alpha}{dt} = \underbrace{\frac{V_0 - v_\alpha(t)}{\tau}}_{\text{Acceleration}} + \underbrace{f_{\alpha(\alpha+1)}(r_\alpha, v_\alpha, r_{\alpha+1}, v_{\alpha+1})}_{\text{Deceleration}} + \xi_\alpha(t). \quad (26)$$

It is known that models of this kind are able to describe the emergence of stop-and-go traffic [5], [4] (cf. Figure 6).

The advantage of the social force concept is, that it allows a very intuitive modelling of decision processes which are related to continuous changes in some (possibly abstract) space of behavioral alternatives [27]. According to this, the different motivations which influence an individual at the same time, are described by additive, force-like quantities. These generalized forces are, of course, no Newtonian forces. For example, they do not obey the law *actio = reactio*. The social force concept is well compatible with theoretical concepts from the social sciences and has been elaborated in detail [27], [5]. It has already been successful in describing various self-organization phenomena in pedestrian crowds [5], [28], but it was also applied to opinion formation processes [27], [29].

In the case of driver behavior, we have two conflicting motivations: On the one hand, the driver likes to accelerate towards his desired velocity V_0 . On the other hand, he wants to keep a safe distance to the car in front. The latter is described by a repulsive deceleration force $f_{\alpha(\alpha+1)}$. Effects $f_{\alpha\beta}$ of interactions with other vehicles $\beta \neq (\alpha + 1)$ have been assumed to be negligible, here. However, they could easily be included in accordance with Eq. (2).

As Fig. 7 shows, a good agreement with empirical data of driver-vehicle behavior can be achieved with the following form of the repulsive interaction force:

$$f_{\alpha(\alpha+1)} := \frac{V'_e(r_{\alpha+1} - r_\alpha) - V_0}{\tau} + f'_{\alpha(\alpha+1)} \quad (27)$$

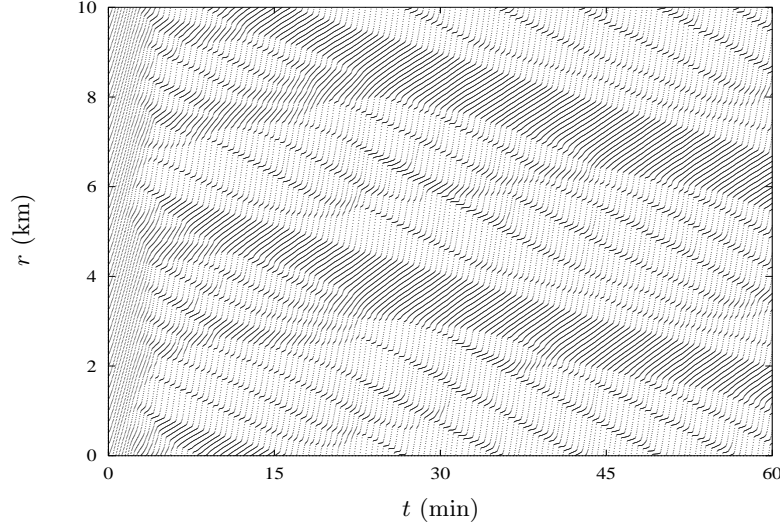


Fig. 6. Representation of the vehicle trajectories of each 10th car on a circular road [5]. The slopes of the trajectories indicate the respective vehicle velocities, whereas their density reflects the spatial vehicle density. The simulation starts with a homogeneous traffic situation (i.e. all vehicles have initially the same distance to the car in front). In the course of time, density clusters emerge. These are often called ‘phantom traffic jams’, since they do not originate from any localized bottleneck.

with

$$f'_{\alpha(\alpha+1)} := -\exp\left(-\frac{r_{\alpha+1} - r_{\alpha} - s(v_{\alpha})}{R}\right) \frac{v_{\alpha} - v_{\alpha+1}}{\tau'} \Theta(v_{\alpha} - v_{\alpha+1}). \quad (28)$$

Here, $\Theta(\Delta v)$ is the Heaviside step function.

If we would restrict the model to the first term of (27) (i.e. in the case $\tau' \rightarrow \infty$), we would arrive at the microsimulation model by Bando et al. [4]. $V'_e(\Delta r)$ is the equilibrium velocity, which is a function of the distance $\Delta r := r_{\alpha+1} - r_{\alpha}$ to the next car ahead. The additional term (28) takes into account that

1. drivers brake stronger, when the relative velocity $\Delta v := v_{\alpha} - v_{\alpha+1}$ is large or when the distance Δr to the car in front is small,
2. the deceleration time τ' is shorter than the acceleration time τ ,
3. drivers begin to brake at a larger distance, if they drive fast. This is described by the velocity-dependence of the safe distance $s(v)$. R is the range of the repulsive effect of a car.

In most microsimulations, the relations $V'_e(\Delta r)$ and parameters τ , τ' , R are specified individually (i.e. in an α -dependent way).

It can be shown that the above force model is consistent in the limiting cases. For large distances or $v_{\alpha} \approx v_{\alpha+1}$, vehicle α approaches the distance-dependent

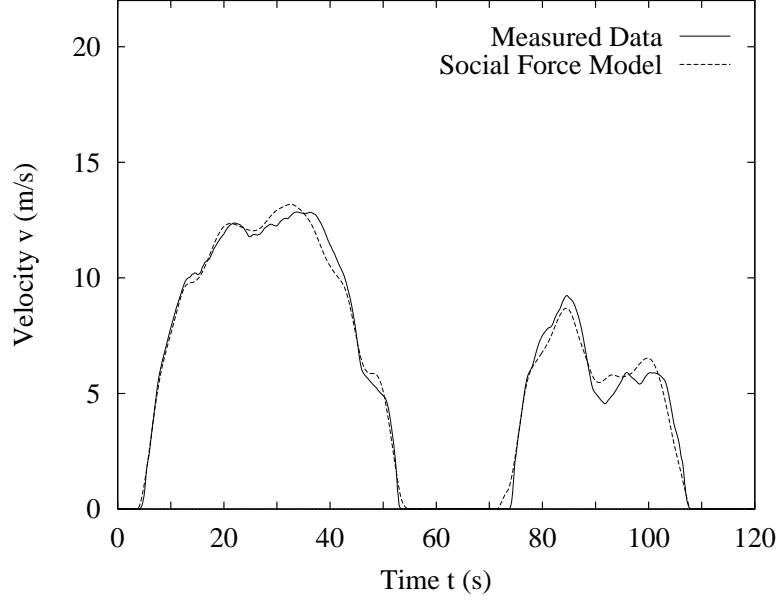


Fig. 7. Time-dependent velocity of a car which follows another car in city traffic. The simulation results for the social force model treat the velocity of the vehicle ahead and its initial distance as given. We find a good agreement with the empirical follow-the-leader data.

equilibrium velocity V'_e :

$$\frac{dv_\alpha}{dt} \approx \frac{V'_e(r_{\alpha+1} - r_\alpha) - v_\alpha(t)}{\tau} + \xi_\alpha(t). \quad (29)$$

For small distances and $v_\alpha > v_{\alpha+1}$, it decelerates to the velocity $v_{\alpha+1}$ of the car in front:

$$\frac{dv_\alpha}{dt} \approx \frac{v_{\alpha+1}(t) - v_\alpha(t)}{\tau' e^{[r_{\alpha+1} - r_\alpha - s(v_\alpha)]/R}} + \xi_\alpha(t). \quad (30)$$

With decreasing distance it brakes stronger.

3.2 Derivation of Macroscopic Traffic Equations

In the following, we write the acceleration relation in the form

$$\frac{dv}{dt} = f(\Delta r, v, w) + \xi(t) := \frac{V'_e(\Delta r) - v}{\tau} + f'(\Delta r, v, w) + \xi(t) \quad (31)$$

with the abbreviations $v := v_\alpha$, $w := v_{\alpha+1}$, $\Delta r := r_{\alpha+1} - r_\alpha$, $\xi := \xi_\alpha$, and

$$f' := f'_{\alpha(\alpha+1)} = f_{\alpha(\alpha+1)} + \frac{V_0 - V'_e(\Delta r)}{\tau}. \quad (32)$$

Relation (31) is now inserted into the kinetic equation

$$\frac{\partial \tilde{\rho}}{\partial t} + \frac{\partial(\tilde{\rho}v)}{\partial r} + \frac{\partial(\tilde{\rho}f)}{\partial v} = \left(\frac{\partial \tilde{\rho}}{\partial t} \right)_{\text{fl}}, \quad (33)$$

which is again a direct consequence of definition (1). Note that the interaction effects were absorbed into the function f , here. Next, we multiply this equation with v^k and $P'(w, \Delta r|v, r, t)$, which denotes the probability that, given a car with velocity v is located at place r , the car in front drives with velocity w at a distance Δr . Finally, the resulting equation is integrated with respect to w and Δr . This gives the macroscopic equations

$$\frac{\partial \rho}{\partial t} + \frac{\partial(\rho V)}{\partial r} = 0, \quad (34)$$

$$\frac{\partial(\rho V)}{\partial t} + \frac{\partial}{\partial r}[\rho(V^2 + \theta)] = \frac{\rho}{\tau}(V_e^* - V) + \rho \mathcal{F}_1, \quad (35)$$

$$\frac{\partial}{\partial t}[\rho(V^2 + \theta)] + \frac{\partial}{\partial r}[\rho(V^3 + 3V\theta)] = \frac{2\rho}{\tau}(V_e^*V + \tau D - V^2 - \theta) + \rho \mathcal{F}_2 \quad (36)$$

with

$$\begin{aligned} \mathcal{F}_k(r, t) &:= k \int d\Delta r \int dv \int dw v^{k-1} f'(\Delta r, v, w) P'(\Delta r, w|r, v, t) \frac{\tilde{\rho}(r, v, t)}{\rho(r, t)} \\ &= -k \int d\Delta r \int dv \int_{w < v} dw v^{k-1} \exp\left(-\frac{\Delta r - s(v)}{R}\right) \frac{v - w}{\tau'} \\ &\quad \times P'(\Delta r, w|r, v, t) P(v; r, t) \end{aligned} \quad (37)$$

and

$$V_e^* := \int d\Delta r \int dv \int dw V_e'(\Delta r) P'(\Delta r, w|r, v, t) P(v; r, t). \quad (38)$$

To get (37), we made use of partial integration.

In the following, we will apply the factorization approximation

$$P'(\Delta r, w|r, v, t) \approx P_*(\Delta r; r, t) P(w; r + \Delta r, t), \quad (39)$$

which is even exact, if the distributions of the velocities w and the headways Δr are statistically independent, and independent of v . Furthermore, we assume that the headway distribution $P_*(\Delta r; r, t)$ is a function of the density ρ and average velocity V at a certain place $r + \delta r$ between r and $r + \Delta r$:

$$P_*(\Delta r; r, t) \equiv P_*(\Delta r; \rho(r + \delta r, t), V(r + \delta r, t)). \quad (40)$$

Then, we can expand (37) and (40) in the small quantities $\delta v := v - V$ and δr , respectively. In this way, we obtain

$$\begin{aligned} \mathcal{F}_k(r, t) \approx & -k \int d\Delta r \int dv \int_{w < v} dw v^{k-1} \frac{v-w}{\tau'} \exp\left(-\frac{\Delta r - s(V)}{R}\right) \left\{ \frac{ds}{dV} \frac{\delta v}{R} \right. \\ & \left. + \frac{1}{2} \left[\frac{d^2 s}{dV^2} + \left(\frac{ds}{dV} \right)^2 \right] \frac{\delta v^2}{R^2} \right\} P_*(\Delta r; r, t) P(w; r + \Delta r, t) P(v; r, t) \end{aligned} \quad (41)$$

and

$$\begin{aligned} P_*(\Delta r; r, t) \approx & P_*(\Delta r; \rho(r, t), V(r, t)) + \frac{\partial P_*}{\partial \rho} \left(\frac{\partial \rho}{\partial r} \delta r + \frac{\partial^2 \rho}{\partial r^2} \frac{\delta r^2}{2} \right) \\ & + \frac{\partial P_*}{\partial V} \left(\frac{\partial V}{\partial r} \delta r + \frac{\partial^2 V}{\partial r^2} \frac{\delta r^2}{2} \right), \end{aligned} \quad (42)$$

where we again neglected products of partial derivatives $\partial g / \partial r$. After carrying out the integrations over v , w , and Δr , the resulting macroscopic traffic equations can again be written in the form of Eqs. (21) to (23). However, the coefficients a_i , b_i , c_i , and d_i are different, since we did not apply the approximation of sudden deceleration maneuvers. The problem of this method is, that it does not provide the functional form of the headway distribution $P_*(\Delta r; \rho, V)$, which is needed for the explicit evaluation of the coefficients. Nevertheless, the use of the above results will be presented by a simple example.

3.3 Relation between Bando's microscopic and Payne's macroscopic traffic model

The microsimulation model by Bando et al. [4] is obtained by neglecting the fluctuation term and the second term in (27), i.e. by setting $D := 0$ and $f' := 0$. In order to calculate the corresponding macroscopic traffic equations, we make a very simple assumption, here, namely that the headways Δr are given by the inverse of the density:

$$P_*(\Delta r; r, t) := \delta \left(\Delta r - \frac{1}{\rho(r + \delta r, t)} \right). \quad (43)$$

Inserting this into the above equations, we finally arrive at the continuity equation

$$\frac{\partial \rho}{\partial t} + V \frac{\partial \rho}{\partial r} = -\rho \frac{\partial V}{\partial r}, \quad (44)$$

the velocity equation

$$\begin{aligned} \frac{\partial V}{\partial t} + V \frac{\partial V}{\partial r} \approx & -\frac{1}{\rho} \frac{\partial(\rho \theta)}{\partial r} + \frac{1}{\tau} \left[V_e^* \left(\frac{1}{\rho} \right) - V \right] - \frac{1}{\tau \rho^2} \frac{\partial V_e^*}{\partial \Delta r} \left(\frac{\partial \rho}{\partial r} \delta r + \frac{\partial^2 \rho}{\partial r^2} \frac{\delta r^2}{2} \right) \\ \approx & -\frac{1}{\rho} \frac{\partial(\rho \theta)}{\partial r} + \frac{1}{\tau} [V_e(\rho) - V] + \frac{1}{\tau} \frac{\partial V_e}{\partial \rho} \left(\frac{\partial \rho}{\partial r} \delta r + \frac{\partial^2 \rho}{\partial r^2} \frac{\delta r^2}{2} \right), \end{aligned} \quad (45)$$

and the variance equation

$$\frac{\partial \theta}{\partial t} + V \frac{\partial \theta}{\partial r} = -2\theta \frac{\partial V}{\partial r} - \frac{2}{\tau} \theta, \quad (46)$$

where

$$V_e(\rho) := V_e^* \left(\frac{1}{\rho} \right). \quad (47)$$

Close to the equilibrium solution, the variance equation can be neglected due to $\theta \approx 0$. The instability condition of the remaining equations (44) and (45) reads

$$\rho \left| \frac{dV_e}{d\rho} \right| \stackrel{!}{>} \frac{\delta r}{\tau} \quad (48)$$

(cf. [5], [13]). This is only compatible with the instability condition

$$\frac{dV_e^*}{d\Delta r} \stackrel{!}{>} \frac{1}{2\tau} \quad \text{or} \quad \rho^2 \left| \frac{dV_e}{d\rho} \right| \stackrel{!}{>} \frac{1}{2\tau} \quad (49)$$

of the Bando model [4], if we choose

$$\delta r \stackrel{!}{=} \frac{1}{2\rho} \approx \frac{\Delta r}{2}, \quad (50)$$

which is very plausible. In this case, the macroscopic equations (44) and (45) agree with the traffic model by Payne [10], but they contain the additional term $[\delta r^2/(2\tau)](\partial V_e/\partial \rho)\partial^2 \rho/\partial r^2$, which describes a smoothing of sudden spatial changes in density and velocity. However, as soon as the approximation $\theta \approx 0$ becomes invalid, Payne's model does not anymore reflect the traffic dynamics according to Bando's model.

4 Summary and Conclusions

We have presented microscopic and macroscopic traffic flow models for freeways, which were successfully confronted with empirical data (cf. also [5], [13], [14]). Moreover, it has been shown, how macroscopic traffic models can be systematically derived from the equations of motion for single vehicles. This is essential for increasing the speed of traffic simulations. Apart from the kinetic approach to this problem, which based on the assumption of sudden deceleration maneuvers, an alternative method has been proposed, which presupposes a suitable approximation of the headway distribution function. The resulting macroscopic traffic equations are related to the hydrodynamic equations of ordinary fluids, but they contain a number of additional terms for three reasons:

1. Vehicles accelerate to a certain desired velocity.
2. A finite equilibrium variance of vehicle velocities is caused by imperfect driving.

3. Vehicle interactions are anisotropic and do not conserve energy or momentum.

The additional terms are responsible for certain instabilities of traffic flow, causing ‘phantom traffic jams’ or ‘stop-and-go traffic’. They are also the origin of viscosity effects and of the divergence of ‘traffic pressure’ at maximum vehicle density. Here, it is essential that vehicular space requirements are taken into account [5], [13], [26]. Otherwise, the macroscopic traffic model would neglect certain characteristic terms, which would limit its validity to non-congested traffic situations.

For the purpose of computer simulations, it is advantageous to have the macroscopic traffic equations in flux representation. This has been analytically derived, but it contains the Gaussian error function. In contrast to previous results [26], the corresponding equations are not restricted to cases of small gradients.

Acknowledgments

The author wants to thank Martin Treiber, Tilo Schwarz, and Benno Tilch for providing Figs. 5, 6, and 7, respectively. He is also grateful to Henk Taale and the Dutch Ministry of Transport, Public Works and Water Management as well as to Thomas Bleile and the Robert Bosch GmbH for providing the empirical data shown in Figs. 1 to 3, and 7, respectively. The presented work has been financially supported by the DFG, Heisenberg scholarship He 2789/1-1, and by the BMBF, grant no. 13N7092 (collaborative research project “SANDY”).

References

- [1] Gazis D.C., Herman, R., Rothery R.W. (1961): Nonlinear Follow the Leader Models of Traffic Flow. *Operations Research* **9**, 545–567
- [2] May A.D., Jr., Keller H.E.M. (1967): Non-Integer Car-Following Models. *Highway Research Record* **199**, 19–32
- [3] Wiedemann R. (1974): *Simulation des Straßenverkehrsflusses* (Heft 8 der Schriftenreihe des IfV, Institut für Verkehrswesen, Universität Karlsruhe)
- [4] Bando M., Hasebe K., Nakayama A., Shibata A., Sugiyama Y. (1995): Dynamical Model of Traffic Congestion and Numerical Simulation. *Phys. Rev. E* **51**, 1035–1042
- [5] Helbing D. (1997): *Verkehrsdynamik: Neue physikalische Modellierungskonzepte* (Springer, Berlin)
- [6] Schreckenberg M., Schadschneider A., Nagel K., Ito N. (1996): Discrete Stochastic Models for Traffic Flow. *Phys. Rev. E* **51**, 2939–2949.
- [7] Nagel K., Paczuski M. (1995): Emergent Traffic Jams. *Phys. Rev. E* **51**, 2909–2918
- [8] Nagatani T. (1995): Bunching of Cars in Asymmetric Exclusion Models for Freeway Traffic. *Phys. Rev. E* **51**, 922–928
- [9] Krauss S., Wagner P., Gawron C. (1996): Continuous Limit of the Nagel-Schreckenberg Model. *Phys. Rev. E* **54**, 3707–3712

- [10] Payne H.J. (1971): Models of Freeway Traffic and Control. In: Bekey G.A. (ed.) *Mathematical Models of Public Systems, Vol. 1* (Simulation Council, La Jolla, CA), 51–61
- [11] Kerner B.S., Konhäuser P. (1994): Structure and Parameters of Clusters in Traffic Flow. *Phys. Rev. E* **50**, 54–83
- [12] Kerner B.S., Konhäuser P., Schilke M. (1995): Deterministic Spontaneous Appearance of Traffic Jams in Slightly Inhomogeneous Traffic Flow. *Phys. Rev. E* **51**, 6243–6246
- [13] Helbing D. (1996): Derivation and Empirical Validation of a Refined Traffic Flow Model. *Physica A* **233**, 253–282
- [14] Helbing D. (1997): Empirical Traffic Data and their Implications for Traffic Modeling. *Phys. Rev. E* **55**, R25–R28
- [15] Prigogine I., Herman R. (1971): *Kinetic Theory of Vehicular Traffic* (Elsevier, Amsterdam)
- [16] Paveri-Fontana S.L. (1975): On Boltzmann-like Treatments for Traffic Flow. A Critical Review of the Basic Model and an Alternative Proposal for Dilute Traffic Analysis. *Transportation Research* **9**, 225–235
- [17] Helbing D. (1996): Gas-Kinetic Derivation of Navier-Stokes-Like Traffic Equations. *Phys. Rev. E* **53**, 2366–2381
- [18] Wagner C., Hoffmann C., Sollacher R., Wagenhuber J., Schürmann B. (1996): Second Order Continuum Traffic Flow Model. *Phys. Rev. E* **54**, 5073–5085
- [19] Helbing D., Greiner A. (1997): Modelling and Simulation of Multilane Traffic Flow. *Phys. Rev. E* **55**, 5498–5508
- [20] Helbing D. (1997): Modeling Multi-Lane Traffic Flow with Queuing Effects. *Physica A* **242**, 175–194
- [21] Chapman S., Cowling T.G. (1970): *The Mathematical Theory of Nonuniform Gases* (3rd edition, Cambridge University Press, Cambridge)
- [22] Jenkins J.T., Richman M.W. (1985): Kinetic Theory for Plane Flows of a Dense Gas of Identical, Rough, Inelastic, Circular Disks. *Phys. of Fluids* **28**, 3485–3494
- [23] Lun C.K.K., Savage S.B., Jeffrey D.J., Chepurin N. (1984): Kinetic Theories for Granular Flow: Inelastic Particles in Couette Flow and Slightly Inelastic Particles in a General Flowfield. *J. Fluid. Mech.* **140**, 223–256
- [24] Goldshtein A., Shapiro M. (1995): Mechanics of Collisional Motion of Granular Materials. Part 1. General Hydrodynamic Equations. *J. Fluid. Mech.* **282**, 75–114
- [25] Helbing D. (1997): Fundamentals of Traffic Flow. *Phys. Rev. E* **55**, 3735–3738
- [26] Helbing D. (1997): Structure and Instability of Consistent High-Density Equations for Traffic Flow. *Phys. Rev. Lett.*, submitted
- [27] Helbing D. (1995): *Quantitative Sociodynamics. Stochastic Methods and Models of Social Interaction Processes* (Kluwer Academic, Dordrecht)
- [28] Helbing D., Molnár P. (1995): Social Force Model for Pedestrian Dynamics. *Phys. Rev. E* **51**, 4282–4286
- [29] Helbing D. (1993): Boltzmann-like and Boltzmann-Fokker-Planck Equations as a Foundation of Behavioral Models. *Physica A* **196**, 546–573

For further references cf. [5].